Engineering and Technology Journal
Journal homepage: https://etj.uotechnology.edu.iq

A Survey on Microstrip Single/Multiband Bandpass Filter for 5G Applications

Halah I. Khani*, Ahmed S. Ezzulddin

Electrical Engineering Dept., University of Technology-Iraq, Alsina'a street, 10066 Baghdad, Iraq.
*Corresponding author Email: eee.19.22@grad.uotechnology.edu.iq

HIGHLIGHTS

- Present various design techniques for present and future 5G applications.
- Presents and discusses a comparison of alternative design techniques and layouts while focusing on the most important parameters of microstrip BPFs.
- Deriving the major challenges from these reviews, which included the size, performance, and individuality of microstrip BPFs filters.

ARTICLE INFO

Handling editor: Ivan A. Hashim

Keywords:
5G applications; Bandpass Filter; Microstrip; Microwave; Multiband.

ABSTRACT

For a long time, extensive research on microstrip bandpass filters has been documented to meet the standards of modern multiservice wireless communication systems. The multiband bandpass filters (BPF) are required for the receiver front end to function as a single device that caters to many bands at the same time. Planar bandpass filters are particularly promising because of their simplicity of manufacture using printed circuit technology, compactness, and low integration cost. Due to the need for high integration, low cost, and high-speed data transmission, the design and implementation of filters for fifth-generation (5G) mobile communication systems is difficult. This paper presents and discusses a detailed survey of existing research on microstrip single\multiband bandpass filter designs for fifth-generation applications, with a focus on the latest advancements in this research and the difficulties that researchers face. Various designs and techniques were given. A detailed comparison of several design techniques is presented and discussed to offer researchers the benefits and drawbacks of each technique and design that may be of interest to a certain application. Recent microstrip single/multiband BPFs are included in the surveys, which use different design techniques and achieve varying performance for current and future fifth-generation applications.

1. Introduction

Microwave filters are an essential component of receivers. A microwave filter is a two-port network that controls the frequency response at a specific point in a microwave system by transmitting at frequencies within the filter's passband and attenuating at frequencies within the filter's stopband. Because lumped element inductors and capacitors cannot be employed at microwave frequencies, transmission line sections that behave as inductors and capacitors are used. Minimizing filter passband losses is critical because it not only minimizes overall transistor losses but also enhances the noise figure when used with a receiver. The filters' major purposes are to reject unwanted signals outside the filter passband and separate or combine signals based on frequency. The canalized receiver, which uses banks of filters to separate input signals, is a good example of the latter application. Filters are sometimes used for impedance matching as well. Before and after a mixer, filters are employed to minimize spurious signals caused by image frequencies, local oscillator feed-through, noise, and signals in the out-of-frequency band. [1].

Previously, waveguides and coaxial or parallel strip line circuits were used in all microwave equipment. Monolithic microwave integrated circuits (MMICs) have recently been introduced, allowing for the usage of microstrip lines and coplanar strip lines. One advantage of employing microstrips is that they provide an accessible surface for mounting solid-state devices. Microwave energy is transmitted via two conductors. A conductor's efficiency can be maximized by matching its characteristic impedance at each of its endpoints. It is assumed that all impedance elements are lumped constants. However, this changes for lengthy transmission lines that span a wide frequency range. Because the frequency of operation is high, the inductances and capacitances of short lengths of conductors are considered [2].

The bandpass filter is recommended in microwave systems over other types due to its small size, which makes it suitable for a wide range of applications. The bandpass filtering method also improves receiver sensitivity, and provides stability and

http://doi.org/10.30684/etj.2022.135858.1288
Received 15 September 2022; Accepted 25 December 2022; Available online 29 January 2023
2412-0758/University of Technology-Iraq, Baghdad, Iraq

durability [3]. The dimension of the distributed components and the number of suggested resonators define the filter properties in a BPF, which is composed of many coupled resonators. As a result, the majority of microstrip filter minimization approaches aim to reduce one or both of these values. In a bandpass filter, the number of utilized components and the types of resonators specify the filter's characteristics and response [4,5]. Generally, raising the number of filter order, or introducing finite transmission zeros (TZs) at specific frequencies, can improve bandpass filter selectivity, increasing the filter size and higher transmission coefficient; so, inserting TZs is the ideal technique to achieve high selectivity [6].

For microstrip line filters, several structures and approaches have been presented, including combline, hairpin, parallel-coupled-line, step impedance, and stub impedance [7–14]. Using a novel microstrip coupled-line technique, created a compact planar BPF. A filter with a 3 GHz frequency band was built using two λg/4-lines of three parallel-coupled lines. Non-uniform line elements separate the lines, and the filter area is 152.57 mm^2. Another solution uses low-temperature co-fired ceramic [10], whose realization is becoming increasingly achievable due to accurate electromagnetic analysis, allowing for filter structures with small physical dimensions. A physically small BPF may be implemented using planar hairpin resonators. The hairpin filter's design employs a variable coupling effect through the hairpin form with T-feeders presented in [11]. The observed operation frequency is around 0.2 GHz lower than the simulated 5.8 GHz center frequency needed by RFID applications. The resonator size is 320.86 mm^2. Combine filter designs, which benefit from small size and minimal loss, are currently widely employed in a variety of applications [12,13]. [12] describes a new enhanced combine BPF with multiple TZs, two poles, and a size of around 138 mm^2. The filter's center frequency is 1.43 GHz, with 11.51% of fractional bandwidth (Δf), a transmission coefficient of approximately 2.781 dB, and a reflection coefficient of around 18.1 dB. [13] designs and explains an upgraded combline bandpass with stepped impedance with an array of SIRs. The design has the benefit of having no lumped parts and minimal via-hole grounds, making it suitable for multilayer microstrip line deployment. The reflection coefficient and transmission coefficient for the fourth-order design is greater than 17 dB and 2.0 dB, respectively, all while employing a planar with a dimension of 13×9 mm^2.

Fifth Generation (5G) mobile communication is becoming increasingly popular due to the rising need for high data rates [15]. Mobile communications technologies have been developing quickly in recent years. After the previous generations, the 5G mobile network is the next wireless industry standard [16,17]. The goal of 5G wireless technology is to provide greater dependability, ultra-low latency, and larger data throughput. For networks with high activity, 5G systems assist to have decent capacity utilization, which also helps to have enhanced availability. Flexible use of 5G is intended over a variety of radio bands, which can range in frequency from 400 MHz to 90 GHz [18]. 5G applications may not need the whole sub-6 GHz bandwidth with this broad range spectrum, yet the needed channel bandwidth for 5G systems must be between 5 MHz and 0.4 GHz [19,20]. The most desirable portion of the 5G spectrum at 3.5 GHz, which is primarily used internationally and has a bandwidth of up to 100 MHz or even more per operator [18].

The purpose of this study is to survey and compare many different design techniques for microstrip single/multi-band BPFs for 5G applications, with a focus on current achievements and difficulties. These surveys may be classified into five groups based on the number of 5G bands in the BPF, as follows:

- Single-band BPFs
- Dual-band BPFs
- Triple-band BFFs
- Quad-band BFFs
- Mixed-band BPFs.

Depending on the system's needs and limits, each category can be done utilizing a variety of design techniques and structures. All of these aspects will be covered in depth in the next sections of this survey. This survey is organized as follows: Section 2 surveys microstrip single-band BPFs for 5G applications. Section 3 surveys microstrip dual-band BPFs for 5G applications. Section 4 microstrip surveys triple-band BPFs for 5G applications, Section 5 microstrip surveys quad-band BPFs for 5G applications, and Section 6 surveys microstrip mixed-band BPFs for 5G applications, with tables of comparisons between these designs following each section. Finally, Section 7 presents the conclusion of the survey.

2. Microstrip Single-Band BPFs for 5G Applications

Al-Areqi, Nadera Najib, et al., [21] presented microstrip BPF with compact size for 5G wireless communication applications. The proposed design is planned to have a 6.1 GHz resonance frequency. The BPF is made up of quarter wave parallel-coupled line resonators and a small resonator connected between the first and last coupled-line part and the 50 Ω transmission line ports. The analysis was made according to the examination of several substrates with relative permittivity (ε_r) of 2.2, 3.55, 4.70, 10.7, and 11.20. The suggested layout using the substrate that has ε_r of 11.20 improves bandwidth performance. ADS software is used for design and analysis. Figure 1(a), depicts the proposed parallel-coupled line BPF configuration and Figure 1(b) depicts the result.

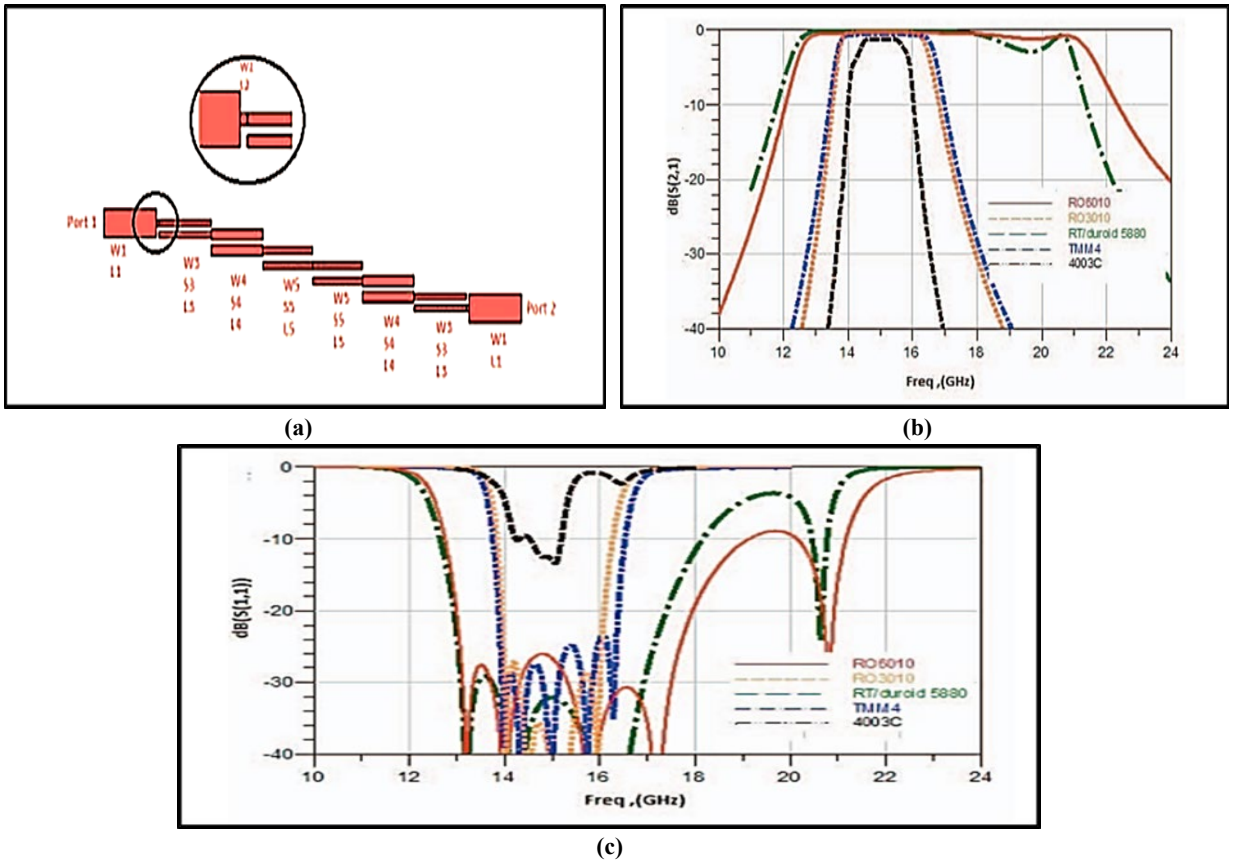

Figure 1: (a)Single-band BPF layout, (b) Simulation S_{21} results,(c) Simulation S_{11} results using different substrates[21]

In 2018, BPF with a small size for 5G wireless communications was proposed by Al-Yasir, Yasir, et al. [22]. The proposed design is planned to have a 3.6 GHz resonance frequency. Three resonators are used in the planar filter, each of which is terminated by a capacitor with input and output terminals with 50Ω transmission line impedances at one end and a via-to-hole ground at the other. Third-order BPF Butterworth properties are achieved at the center frequency by adjusting the coupling between the lines. The suggested combline filter has a very small size of 54 mm^3 and is constructed on an alumina substrate with a ε_r of 9.8. CST software is used to simulate the suggested filter. Figure 2(a) below shows the suggested combline BPF structure and Figure 2(b) shows the simulation results. The resulting designed filter with a small size and extremely low insertion loss makes it an attractive contender for use in 5G spectrum applications.

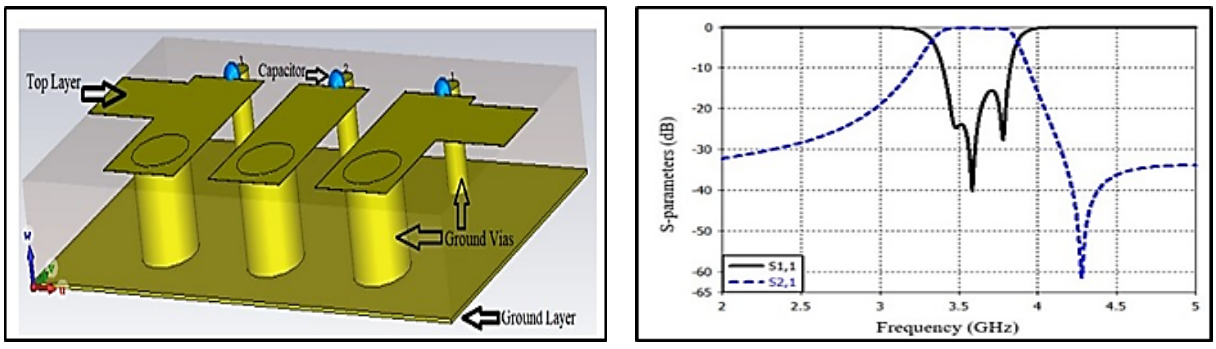

Figure 2: (a) The suggested layout, (b) Simulation results

Microstrip open-loop BPF with a very compact size was proposed by Al-Yasir, Yasir IA, et al., [23] for 5G communication. The proposed design is planned to have a 3.55 GHz resonance frequency. Three trisection open-loop ring resonators and the 50 Ω transmission line ports comprise the planar BPF. To produce a tighter cut-off frequency for the passband, an attenuation zero of finite frequency is successfully constructed on the upper edge of the passband. The implementation of the suggested design not only decreases the design size but also introduces either positive or negative cross-coupling (M_{ij}). Mij between the poles is adjusted for operation in the sub-6 GHz 5G spectrum. CST software is used to simulate the proposed structure and it's constructed on a substrate with a ε_r of 10.2 and a small area of 72.39 mm^3. The simulated and measured findings match well. Figure 3(a), depicts the suggested BPF configuration and Figure 3(b) shows the measured results.

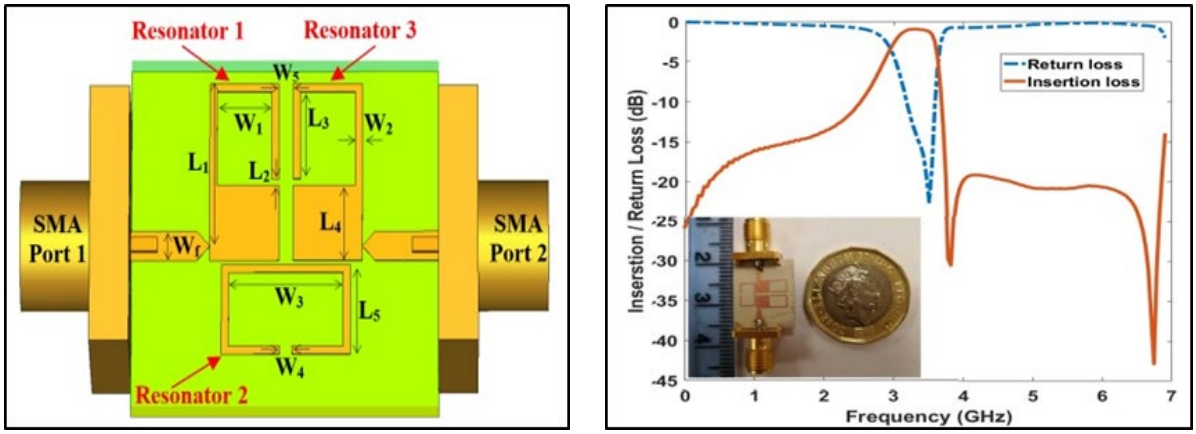

(a) **(b)**

Figure 3: (a) The presented layout, (b) Measured results

Haddi, Souhaila Ben, et al. [17] suggested a compact wideband microstrip BPF by using a rectangular T-Shaped resonator, with excellent performance for the 5G mobile communications systems in 2020. The frequency band also involves the frequencies of the WIMAX and WLAN applications. The proposed design is planned to have a 4.75 GHz resonance frequency with 70% of Δf, a transmission coefficient of less than 1dB, the reflection coefficient of more than 30 dB. The proposed microstrip BPF has a compact size of 45 mm^2 and it has been designed by CST software using an FR4 substrate with a ε_r of 4.3, a thickness of 0.8mm and a tangent loss of 0.025. The results are in good agreement with those produced by ADS software. Figure 4(a) displays the structure of the suggested BPF and Figure4(b) shows the comparison of the simulation results. The suggested filter is easy to fabricate and the outcomes are highly promising.

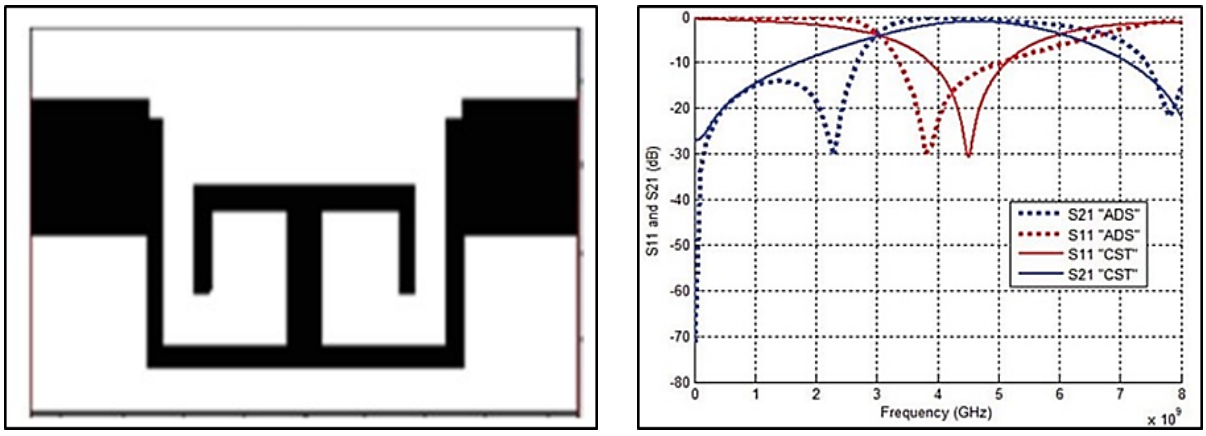

(a) **(b)**

Figure 4: (a) The suggested layout, (b) Simulation results

In the same year, Saleh, Sahar, et al. [24] suggested hairpin BPF (HPBF) and Interdigital BPF (IBF) for 5G wireless communication applications. The proposed design is planned to have 3.95 GHz and 6.55 GHz resonance frequencies. HPBF with a straightforward design had good reflection coefficient and transmission coefficient of 10.43 dB and 0.63 dB, and 14.48 dB and 0.46 dB, respectively, spanning the frequency bands of 3.95 GHz and 6.55 GHz, respectively. Furthermore, to provide great filter performance, IBF can also reduce high-order second harmonics. The simulated reflection coefficient and transmission coefficient are 11.15 dB and 0.63 dB with out-of-band rejection up to 11.12 GHz through the frequency band 3.95 GHz. Additionally, at the second frequency band, IBF is designed with two various groundings via hole radii (rVia), state1: rVia = 0.4 mm and state2: rVia = 0.7 mm. The suggested design performs well in both cases, suppressing high-order second harmonics up to 18.33 GHz and 18.96 GHz. The simulation of this study is carried out using the HFSS software. Figure 5(a) shows the configuration of 3.95 GHz HPBF, Figure 5(b) shows the simulation results of the suggested 3.95 HPBF, Figure 5(c) shows the configuration of 3.95 GHz IBF, and Figure 5(d) shows the simulation results of the suggested 3.95 IBF respectively. Figure 6: (a) shows the structure of 6.55 GHz hairpin BPF, Figure 6(b) shows the simulation results of the suggested 6.55 HPBF, Figure 6 (c) shows the structure of 6.55 GHz Interdigital BPF (state1), Figure 6(d) shows the simulation results of the suggested 6.55 IBF (Case1), Figure 6(e) shows the structure of 6.55 GHz Interdigital BPF (state2), and Figure 6(f) shows the simulation results of the suggested 6.55 IBF (Case2).

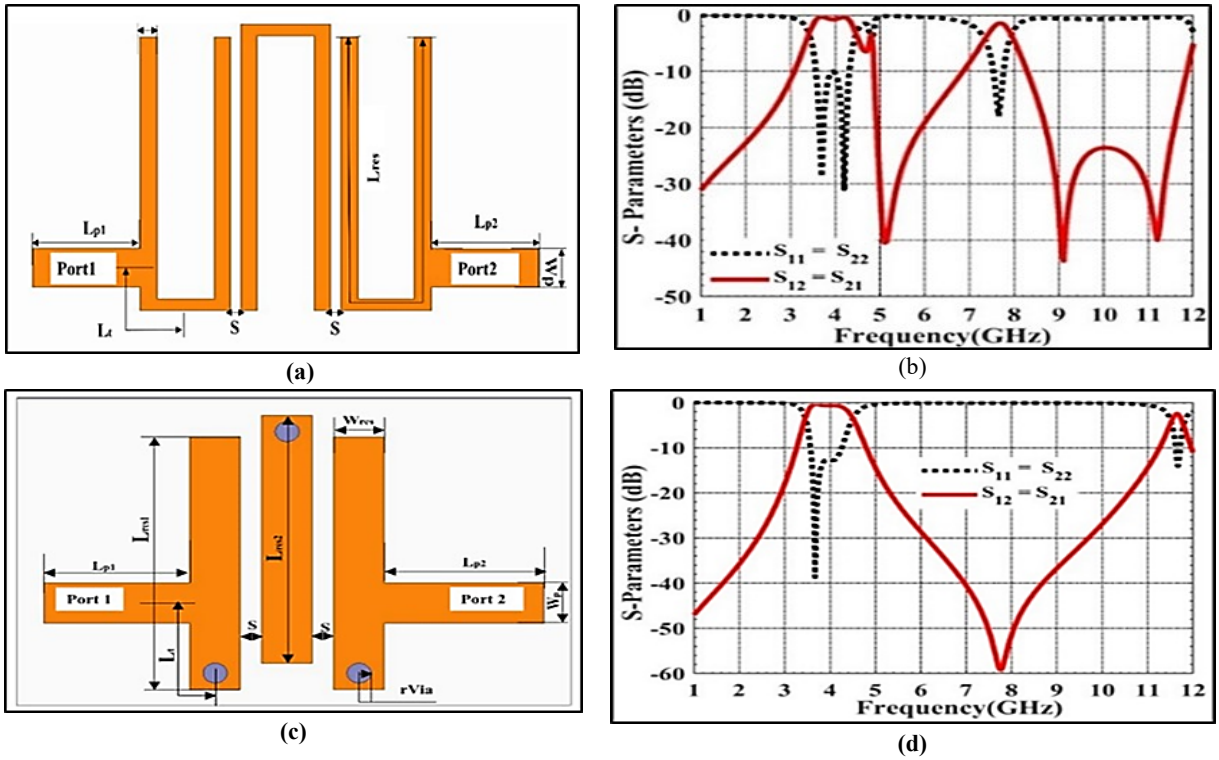

Figure 5: (a) Configuration of 3.95 GHz HPBF, (b) Simulation results of the suggested 3.95 HPBF, (c) Configuration of 3.95 GHz IBF, (d) Simulation results of the suggested 3.95 GHz

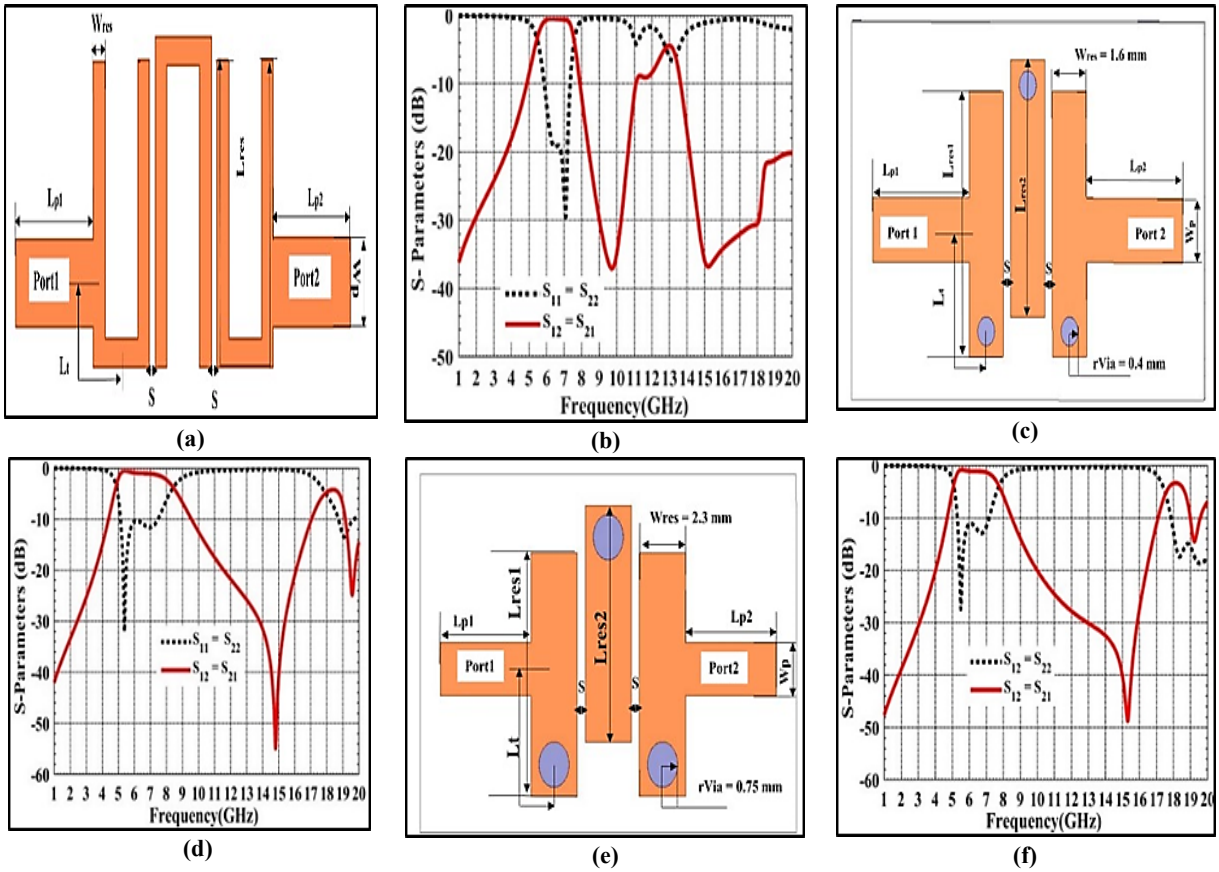

Figure 6: (a) Structure of 6.55 GHz hairpin BPF, (b) Simulation results of the suggested 6.55 HPBF, (c) Structure of 6.55 GHz Interdigital BPF (state1), (d) Simulation results of the suggested 6.55 IBF (Case1), (e) Structure of 6.55 GHz Interdigital BPF (state2), (f) Simulation results of the suggested 6.55 IBF (Case2).

In 2021, Alnahwi, Falih M., et al. [25] presented the design and development of single-band BPF using the SL-MMR technique for 5G applications. Based on a mathematical study of SLRs, the goal of this research is to offer a low-price

microstrip filter with better passband and stopband properties. The suggested filter's cost is decreased by using FR4 dielectric material as a substrate. The odd-mode and even-mode resonant frequencies of the SL-MMR are predicted using mathematical formulas derived from the filter's transmission line model. At the resonance frequency, a Δf of 12.8% has been obtained with a reflection coefficient better than 18 dB and a transmission coefficient lower than 2.5 dB. Additionally, a pair of parasitic elements are attached to the presented structure to provide an extra TZ in the filter's lower stopband to improve filter stopband suppression. The outcomes of the measurements and simulations agree well, and both show that the filter's stopband and passband properties are suitable. Figure 7(a) depicts the suggested BPF prototype, Figure 7(b) shows the S_{11} comparison of measured and simulated, and Figure 7(c) shows the S_{21} comparison of measured and simulated.

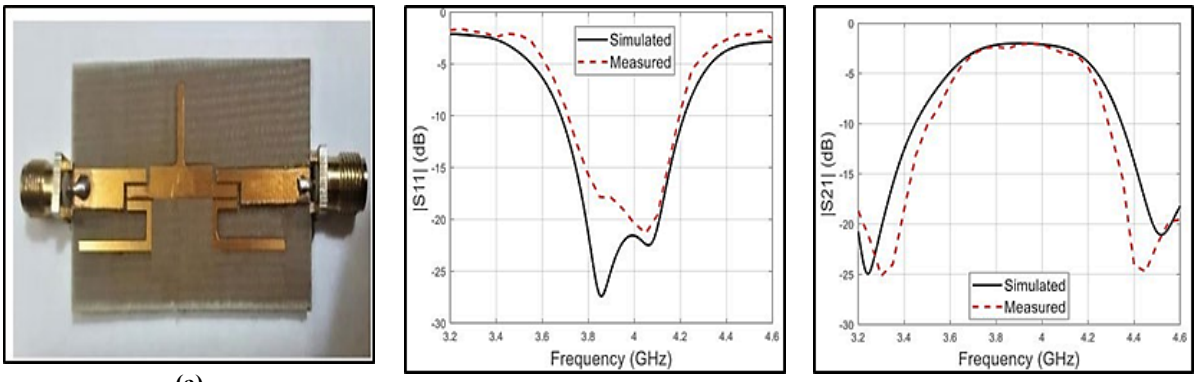

(a) (b) (c)

Figure 7: (a) The prototype of the presented layout, (b) S_{11} comparison of measured and simulated, (c) S_{21} comparison of measured and simulated.

A viable solution for reducing the size of planar microstrip filters is multilayer construction. Multilayer BPF results in greater and improved dimensions due to its flexible design and combination of additional microwave components. Abdullah, Qazwan, et al., [26] proposed a parallel-coupled line (PCL) BPF and multilayer (ML) hairpin BPF for 5G applications. The center frequency and bandwidth of the intended four-pole resonator are 2.58 GHz and 130 MHz, respectively. The filters have a Chebyshev response and a passband ripple of 0.1 dB. The compact filter design structures are offered by the hairpin line. They can theoretically be made by "U" bending λg/2-line resonators with parallel couplings. The ML BPF is created using the parallel-coupled line resonator construction. The substrate utilized was FR4, which has a 1.6 mm thickness and a relative permittivity (ε_r) of 4.3. To verify the effectiveness of the suggested filter design, a comparison between the simulated transmission coefficient and the return loss of substrates RO3003 and FR4 was made. CST software and ADS software are used to simulate the PCL filter. A comprehensive tally between simulation results and measured findings was reached during the experimental validation of the PCL Bandpass filter, proving a precisely measured return loss. The hairpin ML BPF performs well in terms of S-parameter characteristics, according to the simulation findings, and the filter size is greatly decreased. Figure 8(a) displays the suggested BPF prototype Figure 8(b) shows the S_{11} comparison of measured and simulated, and Figure 8(c) shows the S_{21} comparison of measured and simulated.

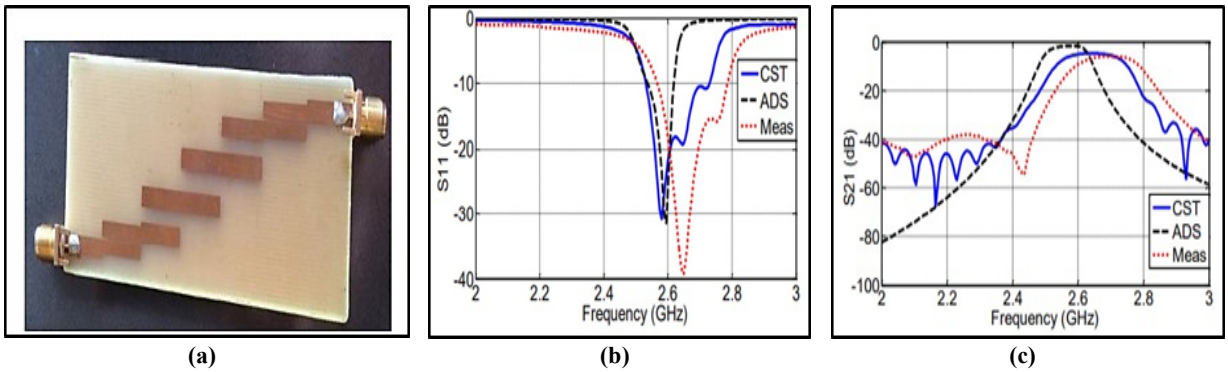

(a) (b) (c)

Figure 8: (a) The fabricated PCL BPF (b) S_{11} comparison of measured and simulated and (c) S_{21} comparison of measured and simulated using FR4.

Basheer, Ameer, et al. [27] suggested a third-order microstrip single-band BPF based on fractal coupled lines and two slotted lines for 5G Applications. The suggested structure has a broadband rejection response and high selectivity properties. HFSS software is used to simulate the suggested design. The filter is built on a substrate that has a thickness of 0.508 mm and an ε_r of 3.55 and is intended to have a resonance frequency of 6.1 GHz. The simulation outcomes display good selectivity, broadband rejection, and a Δf of 8.1%. Figure 9(a) shows the structure of the suggested BPF and Figure 9(b) shows the simulation results. The performance comparisons for recent microstrip single-band BPFs for 5G applications are listed in Table1.

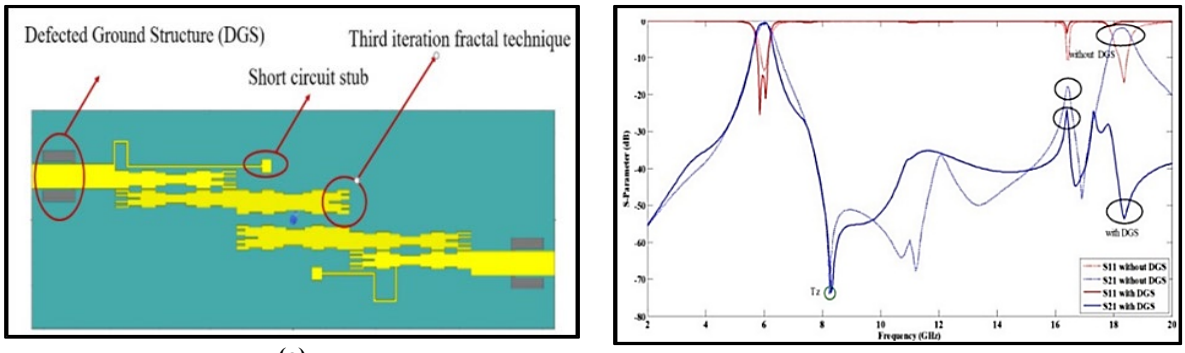

(a) **(b)**

Figure 9: (a) The suggested layout, (b) Simulation results

Table 1: Performance comparisons for recent microstrip single-band BPFs for 5G Applications

Technology	Substrate	Freq. (GHz)	FBW (%)	$\|S_{21}\|$ (dB)	$\|S_{11}\|$ (dB)	Size (λg^2) or(mm^2)	Applications	Ref.
Quarter wave parallel-coupled line	RT/Duroid 5880	15.38	37	0.8	10	139.7 mm^2	5G Wireless Communication	[21]
	RO4003C	15.05	4.33	1.7	10	275.4 mm^2		
	TMM4	15.1	18.6	1.5	10.2	151.42 mm^2		
	RO6010	16.2	44.7	1	10	15.68 mm^2		
	RO3010	15.15	21.73	2	10	94.08 mm^2		
Combline	Alumina	3.6	11	0.1	15	-	5G wireless communications	[22]
Open-loop	RO3010	3.55	8	0.9	22	0.0459 λg^2	5G Communications	[23]
Rectangular T-Shaped	FR4	4.75	3-6	0.9	31	45 mm^2	5G mobile communications systems	[17]
Hairpin	RO4003C	3.95	18.99	0.79	10	-	5G RF front-end wireless communication applications,	[24]
		6.61	22.39	0.5	19			
Interdigital	RO4003C	3.91	17.65	0.63	11.15	-		
		6.31	Case1: 39.93	1	10.32			
		6.23	Case2: 29.9	1.09	11.05			
SIR/SLR	FR4	3.95	14	2.4	19	1250 mm^2	5G Mid-Band Applications	[25]
Hairpin	FR4	2.64	-	5.7	39.24	2766.5 mm^2	5G Applications	[26]
A fractal coupled line with DGS	RO4003C	6.1	8.1	0.6	15	152.65 mm^2	Mobile Telecommunications (IMT) services	[27]

3. Microstrip Dual-Band BPFs for 5G Applications

Riaz, Muhammad, et al. [28] presented a new dual-band BPF construction with excellent selectivity, good isolation, and a broadband rejection for 5G communications systems. The proposed design is planned to have 4.6 GHz and 5.4GHz resonance frequencies with Δf of 13.5% and 11.5%, respectively. The open-loop resonators in the visa-free dual-band filter are shunt loaded with a λg/2-line open-circuit stub. The SIRs, which are inter-digitally coupled to the input/output feed lines, are connected to the resonators through electromagnetic coupling. The resonant mode and TZ frequencies may be changed by adjusting the two stubs' sizes. The performance of the filter is confirmed by the measurement results. The reflection coefficients are more than 20 dB, while the transmission coefficients are 1.02 and 0.8 dB. The filter's skirt steepness is more than 290 dB/GHz, and isolation between bands greater than 35 dB. The suggested design prototype is shown in Figure 10(a), and Figure 10(b) shows the comparison of the simulation and measurement findings.

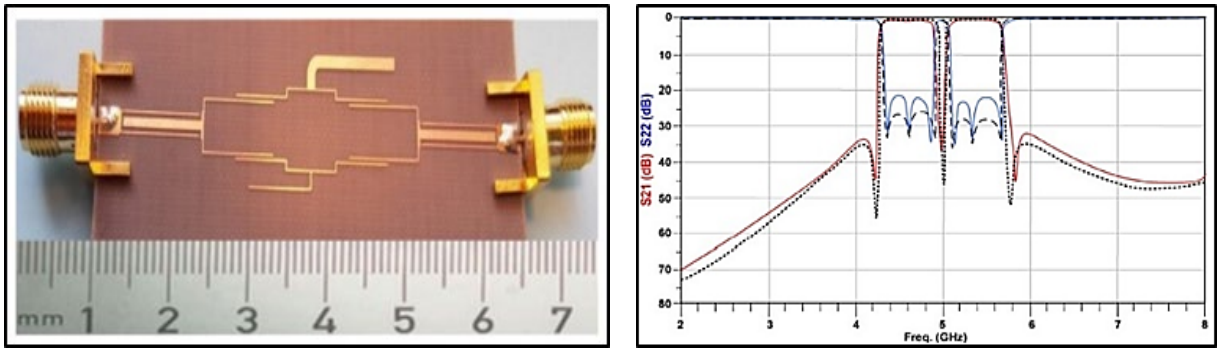

(a) **(b)**

Figure 10: The prototype of the suggested design, (b) Measured and simulated frequency responses comparison

Also in 2020 Hsu, Wei-Lun, et al. [29] provided a compact dual-band BPF with interlocking SIRs created for 5G New Radio Access Technology. The proposed design is planned to have 0.946 GHz and 1.48 GHz resonance frequencies with Δf of 9.8% and 9.5%, respectively which cover six defined ranges in the 5G mid-band range. Three stopbands are needed at 500-850, 1050-1350, and 1600-2000 MHz, respectively. To reach the highest level of merit, an interconnected arrangement of two SIRs is presented. One benefit is that the inter-locked SIR's impedance ratio may be adjusted to have two passbands at the desired frequencies. Second, the coupling part of the interlocked SIR provides three TZs allocated to each stopband, significantly improving stopband suppression. The estimated transmission coefficients and reflection coefficients are 2.16 dB and 1.33 dB, respectively, and the reflection coefficient exceeds 10 dB for the provided design. Stopband suppression is more than 38 dB at the transmission zeros. The circuit is very small, equal to 0.03 λg^2. Figure 11(a) depicts the presented design prototype and Figure 11(b) depicts the comparison of simulation and measured findings.

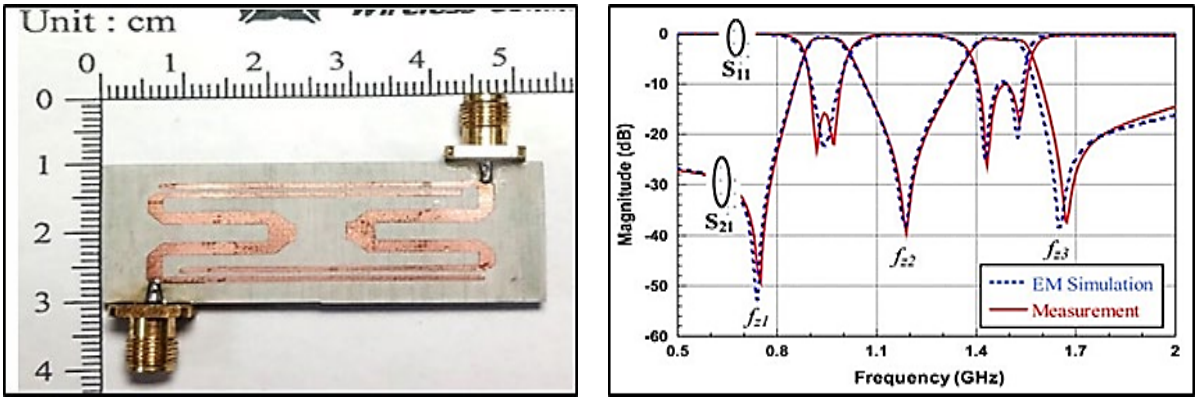

(a) **(b)**

Figure 11: (a)The prototype of the suggested design, (b) Measured and simulated results comparison.

A cross-coupled dual-band BPF with separated electric and magnetic coupling pathways for 5G mid-band applications was presented by Zhang, Wenwen, et al. [30] in the same year. This layout also includes source-to-load couplings to improve the flexibility of heterogeneous feed lines. The dual-band BPF generates a total of five adjustable transmission zeros (TZs). By using two pairs of λg/4 SIRs, the filter achieves high overall performance. The stepped-impedance resonators constituting the second passband are divided and folded onto two different layers to reduce the size of the filter while increasing the controlled range of the second passband. Figure 12(a) shows the prototype of the presented design and Figure 12(b) shows the comparison of the simulation and measured findings. The measured result shows that 7.82% and 4.08% of Δf is achieved, and the resonance frequencies are 3.45 GHz and 4.9 GHz with transmission coefficients of 1.15 and 1.42 dB, respectively.

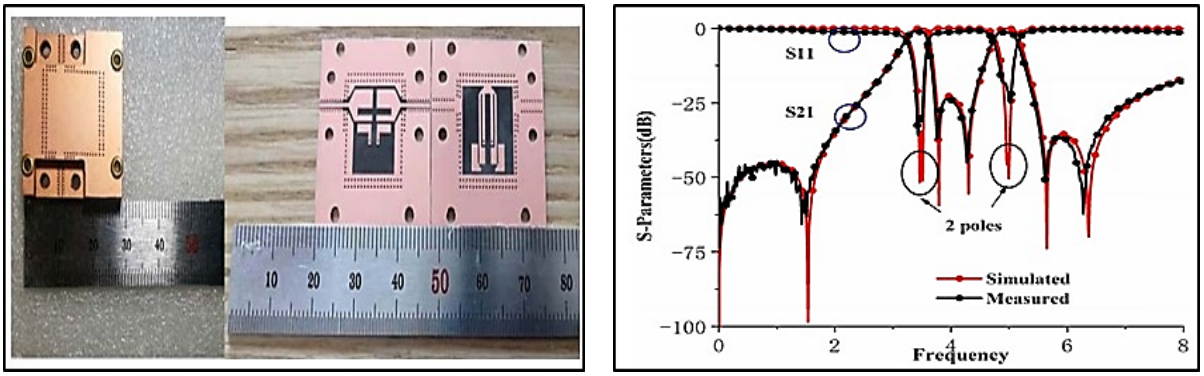

(a) **(b)**

Figure 12: (a) The model of the suggested design, (b) Measured and simulated frequency responses comparison

Later in 2020 Peng, Jinyu, Zhimeng Xu, and Jun Zhu.[31] suggested a compact dual-band BPF by using a folded short-circuited stub-loaded SIR and a uniform impedance resonator (UIR) for 5G communication. The proposed design is planned to have 3.45 GHz and 4.9 GHz resonance frequencies. Because of its hybrid feed scheme, the suggested filter is small and highly independent. Simultaneously, the source load is coupled to produce TZs, which increases the filter's suppression. Furthermore, the loaded rectangular defective ground structure (DGS) may be employed to change the impedance matching, making the design more adaptable. The test confirmed that the provided filter performs well, and the measured findings match well with the simulated results. The suggested design prototype is displayed in Figure 13(a), and Figure 13(b) shows the comparison of the simulation and measurement findings.

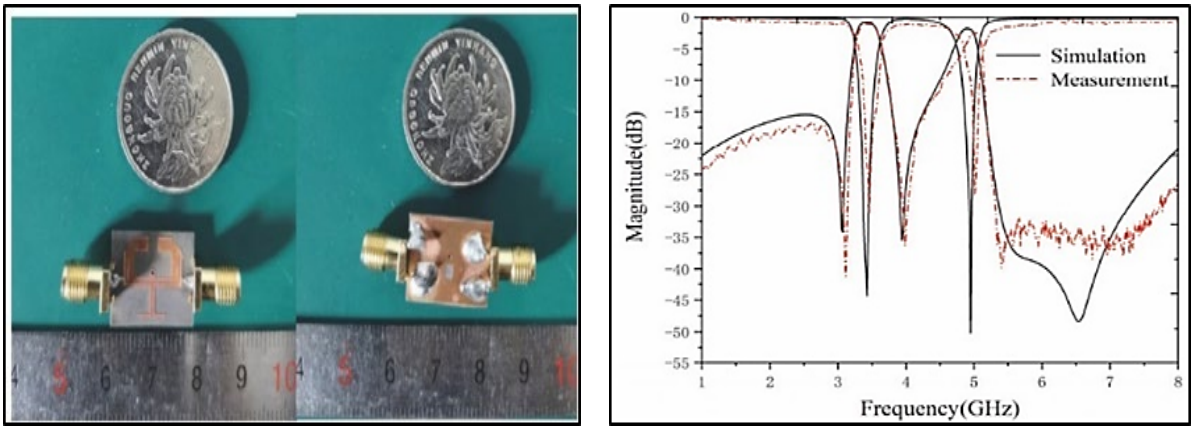

(a) **(b)**

Figure 13: (a) The prototype of the proposed design, (b) Measured and simulated frequency responses comparison.

Based on two folded λg/2-line resonators dual-band BPF is proposed by Khani, Halah I., and Ahmed S. Ezzulddin. 2022, [32] with a quite simple layout, small size, good selectivity, and independent bands for 5G mobile communications. The proposed design is planned to have 3.5 GHz and 5.45 GHz resonance frequencies with Δf of 4.8% and 8.9%, respectively. The filter's resonance frequencies are developed and configured individually. The suggested filter has a transmission coefficient and reflection coefficient of -0.8 dB, -0.5 dB, -20 dB, and -18.4 dB respectively, also four TZs are achieved. The suggested design has a small size of 0.039 λg^2 and is built on a RO4350B substrate with an ε_r of 3.66, and a thickness of 0.508 mm. Figure 14(a) depicts the proposed dual-band BPF configuration and and Figure 14(b) shows the simulation results. The findings of the simulation and LC circuits seemed to be in good match with the theoretical results, as shown in Figure 15(a) for the first band and Figure 15(b) for the second band. The performance comparisons for recent microstrip dual-band BPFs for 5G applications are listed in Table 2.

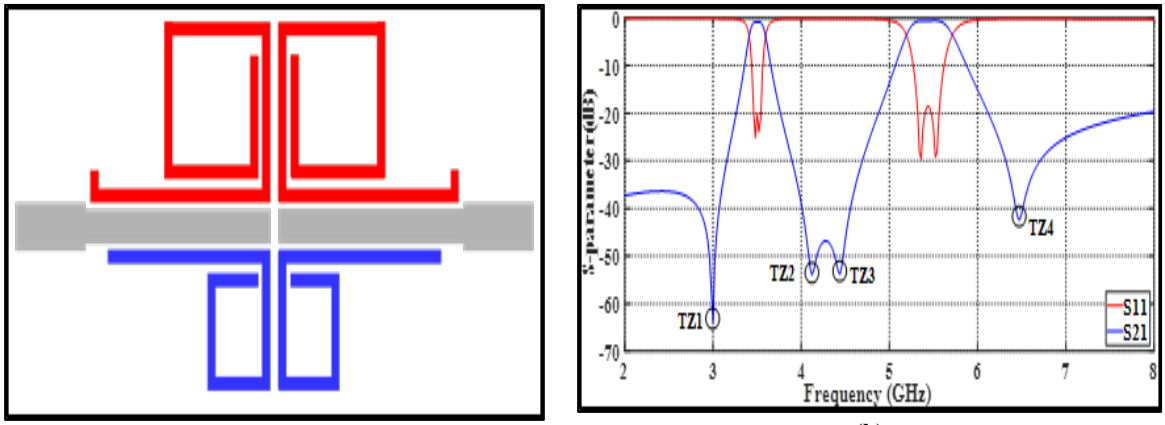

(a) **(b)**

Figure 14: (a) The suggested layout, (b) Simulation findings

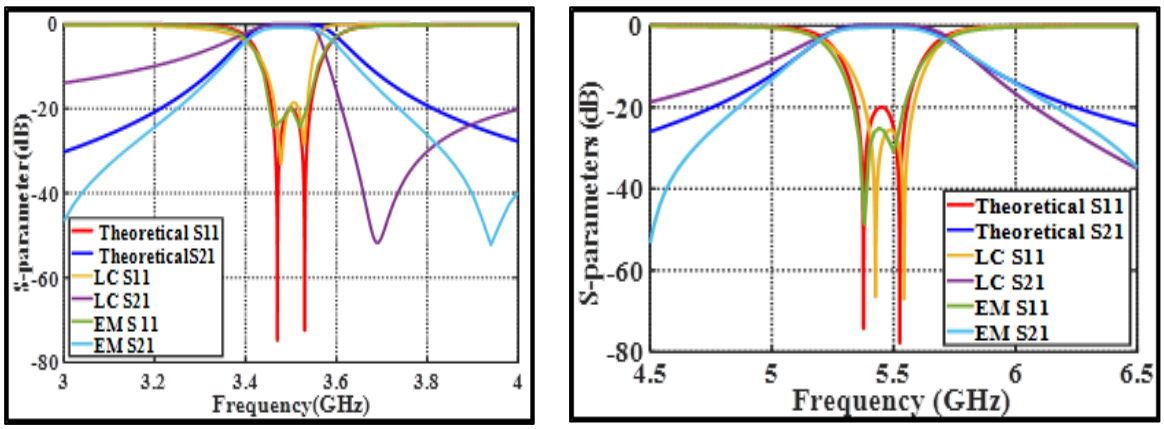

(a) First band **(b) Second band**

Figure 15: Theoretical, EM simulation, and LC circuit findings comparison

Table 2: Performance comparisons for recent microstrip dual-band BPFs for 5G Applications

Technology	Substrate	Freq. (GHz)	FBW (%)	$\|S_{21}\|$ (dB)	$\|S_{11}\|$ (dB)	Size (λg^2) or (mm^2)	IS (dB)	TZs	IBs	Applications	Ref.
coupled lines multimode	Arlon CuClad217LX	4.6\5.4	13.5\11.5	1.02\0.8	>20	-	>-40	3	NA	5G communications systems	[28]
SIR	RO4003C	0.946\1.48	9.8\9.5	2.16\1.26	>10\10	0.03 λg^2	>-40	3	NA	5G new radio access technology	[29]
SISL	RT/duroid5880	3.45\4.9	7.82\4.08	1.15\1.42	>25\<25	0.0651 λg^2	>-50	5	yes	5G Sub-6 GHz Bands	[30]
folded short-circuited stub-loaded step impedance\ uniform impedance	RT5880	3.45\4.9	-	0.9\2.4	31\28	0.0513 λg^2	>-35	3	yes	5G communication	[31]
Folded λg/2-Line	RO4350B	3.5\5.45	4.8\8.9	0.8\0.5	20\18.4	0.039 λg^2	>-50	4	yes	5G mobile communications	[32]

4. Microstrip Triple-Band BPFs for 5G Applications

Hou, Zhanyong, et al., [33] proposed dual-band BPF by using two folded open-loop stepped-impedance resonators (FOLSIRs) and a triple-band BPF by using a pair of folded uniform impedance resonators placed within the dual-band BPF with minimal increase in physical size for 5G mobile communications. The FOLSIR has a more compact construction, a controlled TZ, and an adjustable resonant frequency due to a new structural deformation of a SIR. The measurement results indicate that the operating bands of the two filters are 2.13 GHz /3.47 GHz and 2.17 GHz /3.51 GHz /4.86 GHz, respectively which is compatible with the simulation results. The fabricated filters are small in size, Figure 16(a) show the prototype of the dual-band BPF, Figure 16 (b) shows the comparison of measured and simulated results of the dual-band BPF, Figure 16 (c) shows the prototype of the triple-band BPF,and Figure 16 (d) shows the comparison of measured and simulated results of the triple-band BPF.

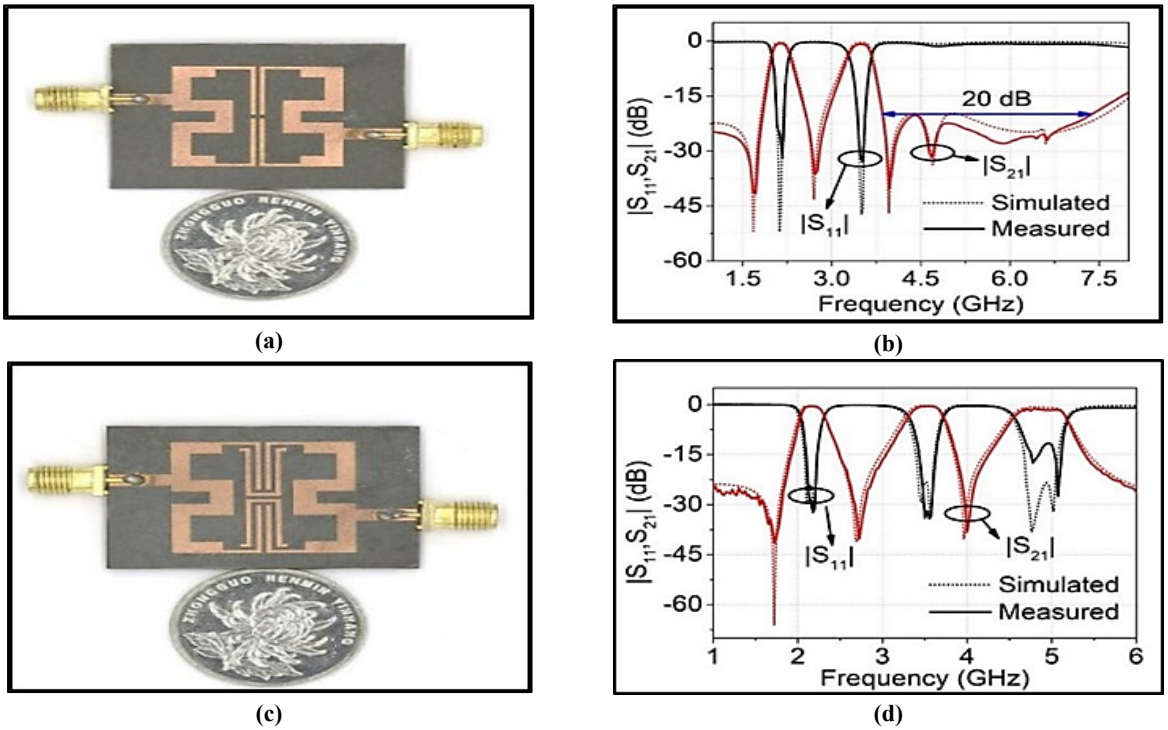

Figure 16: (a) The prototype of the dual-band BPF, (b) Comparison of measured and simulated results, (c) The prototype of the triple-band BPF, (d) Comparison of measured and simulated results.

The essential problem in constructing a multi-band bandpass filter is to ensure that each passband response is extremely independent, allowing each band to be controlled and adjusted independently. Khani, Halah I, et al., [34] propose a triple-band BPF with a compact size, simple construction, and independent bands intended to use for 5G applications. To accomplish the suggested filter performance, two types of resonators are employed. The first resonator is a U-shape. The second and third resonators are folded half-guided wavelength resonators with frequencies of 2.63, 3.43, and 4.66 GHz, respectively. The three

passband frequencies are independently adjustable and designable. A meandering structure is also presented to minimize the size of the proposed filter by 14.04% compared to its prior size. The suggested filter has a transmission coefficient of -1.5 dB, 0 dB, and -1 dB, as well as a reflection coefficient of -15.43 dB, -28.41 dB, and -25.3 dB. Figure 17 (a) shows the prototype of the proposed design, and Figure 17(b) shows that the EM simulation, LC equivalent circuit, and measured findings appear to be in excellent agreement. The performance comparisons for recent microstrip triple-band BPFs for 5G applications are listed in Table 3.

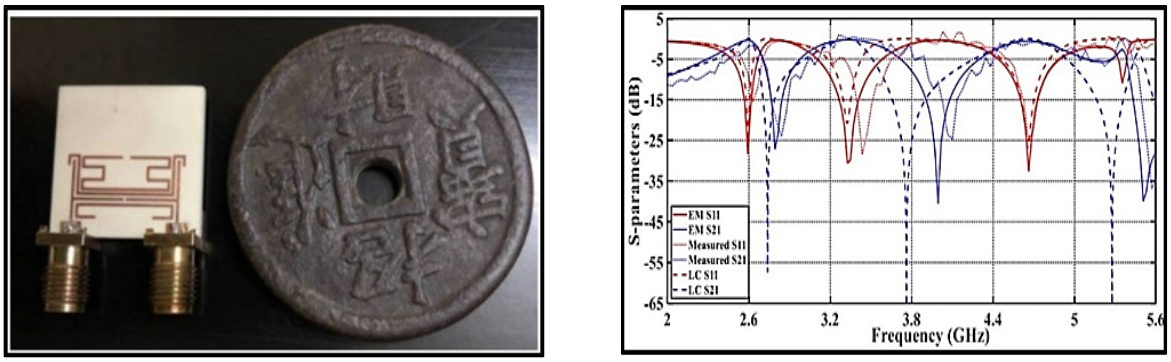

(a) (b)

Figure 17: (a) The prototype of the proposed design, and (b) Comparison of measured, simulated, and LC circuit results.

Table 3: Performance comparisons for recent microstrip triple-band BPFs for 5G Applications

Technology	Substrate	Freq. (GHz)	FBW (%)	$\|S_{21}\|$ (dB)	$\|S_{11}\|$ (dB)	Size (λg^2) or(mm^2)	IS (dB)	TZs	IBs	Applications	Ref.
FOLSIRs	Rogers 5880	2.17/3.51 /4.86	12.4/11.4 /13.3	0.46/0.49 /1.3	32/33/11.6	0.05 λg^2	>-40\>-40	3	yes	5G mobile communications	[33]
U-shape, folded λg/2-line	RO4350B	2.63\3.43 \4.66	-	1.5\0\1	15.43\28.41 \25.3	0.026 λg^2	>-20\>-25	2	yes	5G mobile communications	[34]

5. Microstrip Quad-Band BPFs for 5G Applications

Khani, Halah I, et al. [35] presented a quad-band BPF with excellent selectivity, a small area, and highly independent bands for 5G applications. The described layout comprises two filters. The top filter creating from a short stub-SIR resonator loaded on a C-shape resonator resonating at 2.62 GHz and 3.5 GHz, respectively. The bottom filter is created from two folded L-shape resonators resonating at 4.9 GHz and 6.22 GHz, respectively. The suggested filter has transmission coefficients of 2.7 dB, 0.7 dB, 2.3 dB, and 0.4 dB, as well as reflection coefficients of 13.32 dB, 11.03 dB, 9.17 dB, and 17.89 dB, respectively. Furthermore, eight TZs achieved. The suggested layout is constructed on a substrate with an ε_r of 3.66, and a thickness of 0.508 mm with a size of 0.02 λg^2. Figure 18(a) shows the prototype of the proposed design, and Figure 18(b) shows the comparison of measured and simulated results.

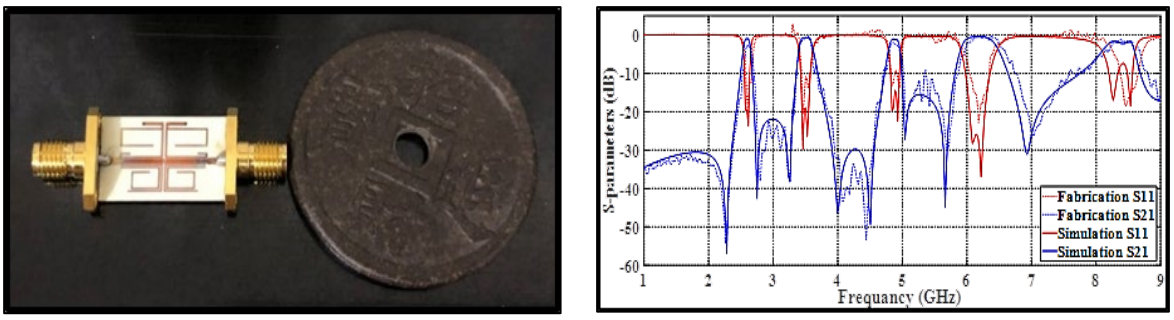

(a) (b)

Figure 18: (a) The prototype of the proposed design, and (b) Comparison of measured and simulated results

6. Microstrip Mixed-Band BPFs for 5G Applications

Hou, Zhanyong, et al. [36] introduced a new compact triple-band BPF with controllable operating frequencies by using a new multi-stub loaded resonator with eight resonance modes. The highest of the three bands is constructed by four modes for the 5G WiFi applications. Two modes are used to actualize the other two passbands, which have resonance frequencies of 2.4 GHz and 3.5 GHz. A prototype filter is used to validate the given idea. Figure 19 exhibits the proposed idea by demonstrating

the good match between the predicted and measured outcomes. Figure 19(a) shows the layout of the proposed design, and Figure 19 (b) shows the comparison of measured and simulated results

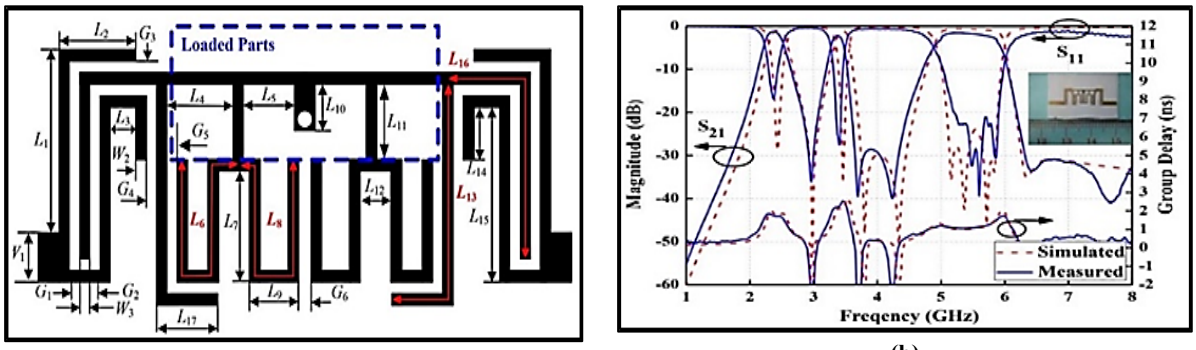

(a) (b)

Figure 19: (a) The layout of the proposed design, and (b) Comparison of measured and simulated results

Zhang, Yao, Li Gao, and Xiu Yin Zhang. [37] proposes a small quad-band BPF for DCS, WLAN, WiMAX, and 5G Wi-Fi applications. It employs two resonators. The first resonator is a multi-stub-loaded with frequencies in the first, second, and fourth passbands. The second resonator is a short-end stub-loaded that generates the third passband. The highest of the four passbands is intended to cover 5G Wi-Fi applications. The suggested quad-band BPF prototype is displayed in Figure 20(a), and Figure 20(b) shows the comparison of the simulation and measurement findings.

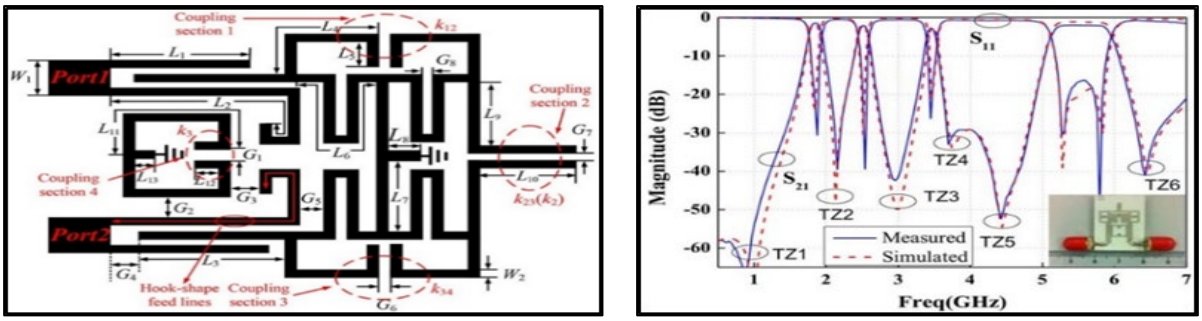

(a) (b)

Figure 20: (a)The prototype of the suggested design, and (b) Measured and simulated results comparison

Khundrakpam, Pinky, et al. [38] suggested a two-order dual-band BPF by using a λg/2 SIR that operates at 2.45 GHz and 5.45 GHz passbands. To enhance coupling, ground slots were implanted below the coupled-line section, resulting in passbands of 0.56 GHz and 0.47 GHz. Four TZs produced near the two passband edges at 1.75 GHz, 3.79 GHz, 6.23 GHz, and 9.34 GHz improved filter selectivity. Figure 21(a) depicts the suggested layout and Figure 21(b) depicts the simulation results.

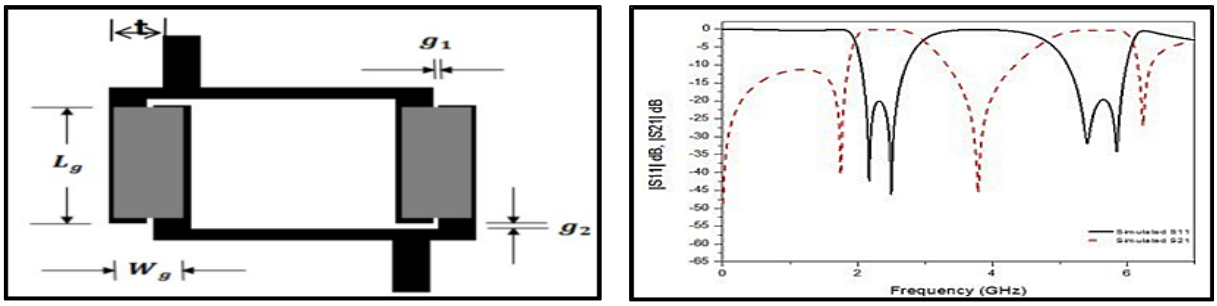

(a) (b)

Figure 21: (a) The suggested dual-band BPF layout; (b) Simulated results

Al-Yasir, Yasir IA, et al. [7] presented an extremely small dual-band BPF by using four open-loop ring resonators for 4G and 5G applications, encompassing the bands 2.55 GHz and 3.65 GHz respectively. One infinite and three finite TZs are successfully constructed on the top and lower edges of the 4G and 5G passbands to obtain sharper cut-off frequencies. The use of four-section resonators decreases the structural size and offers either positive or negative cross-coupling. The cross-coupling coefficients between the resonators are tuned to resonate at the desired frequency and bandwidth. The proposed layout is simulated by CST software and constructed on a substrate with ε_r of 10.2 and a relatively small size of 0.045 λg^2. Figure 22(a) shows the prototype of the suggested design; and Figure 22 (b) shows the measured results. As seen in Figure 22, there is a good match between the simulated and measured findings.

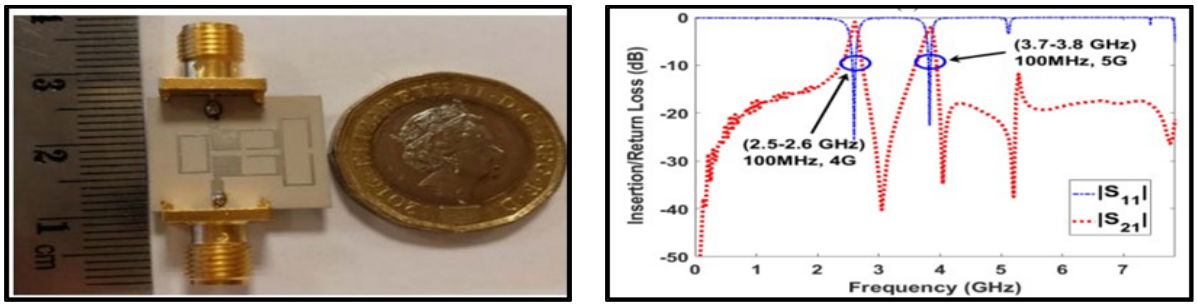

(a) **(b)**

Figure 22: (a) The prototype of the suggested design; (b) The measured results

Lin, Kuan-Jen, et al.[39] presented a compact triple-band BPF by using SL-UIR resonators. Resonators can enable many path propagations to improve filter performance and reduce its size. For WLAN and 5G, the multipath SL-UIRs are built with two resonant paths at 2.4, 3.5, and 5.2GHz. By adjusting the length of the UIRs, the resonant frequencies may be simply regulated. The suggested triple-band filter BPF has a simple design method, a compact circuit size, and a simple structure. Figure 23(a) shows the prototype of the suggested design; and Figure 23 (b) shows the measured and simulated results comparison. The observed results correlate well with the results of the full-wave electromagnetic modeling, as shown in Figure 23.

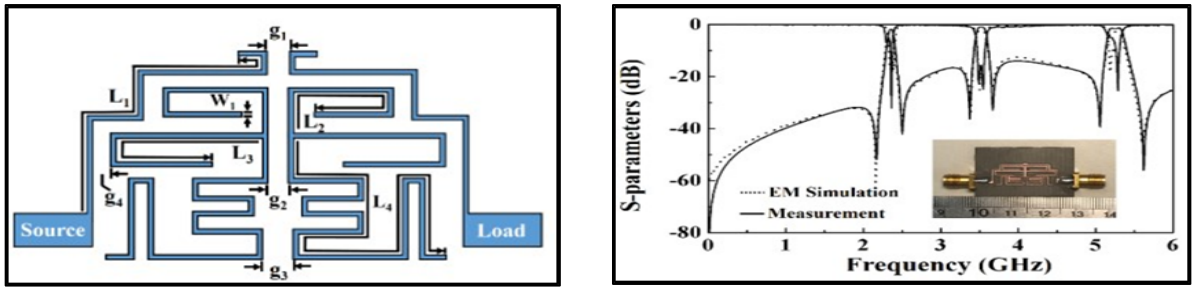

(a) **(b)**

Figure 23: (a) The prototype of the suggested design, and (b) Measured and simulated results comparison

Firmansyah, Teguh, et al. [40] presented triple-band BPF from a folding multicoupled-line and stub-SIR intended for GPS applications at 1.57 GHz, 3G communication at 1.8 GHz, WLAN at 2.4 GHz, 4G communication at 2.6 GHz, and 5G communication at 3.5 GHz. To provide a passband with high independence, the presented design is built as a multicoupled line. Furthermore, the triple-band performance is generated individually and independently by using three resonators. All passband frequencies can be adjusted and designed independently. A folding construction is also presented to miniaturize the triple-band BPF. The consequence is the layout has a small size that is 61.29% smaller than earlier structures. The filter is implemented and tested to investigate and validate the suggested layout of the triple-band BPF. Figure 24(a) shows the prototype of the suggested design; and Figure 24(b) shows the measured and simulated results comparison.. Figure 24 shows a good match between the simulated and measured findings.

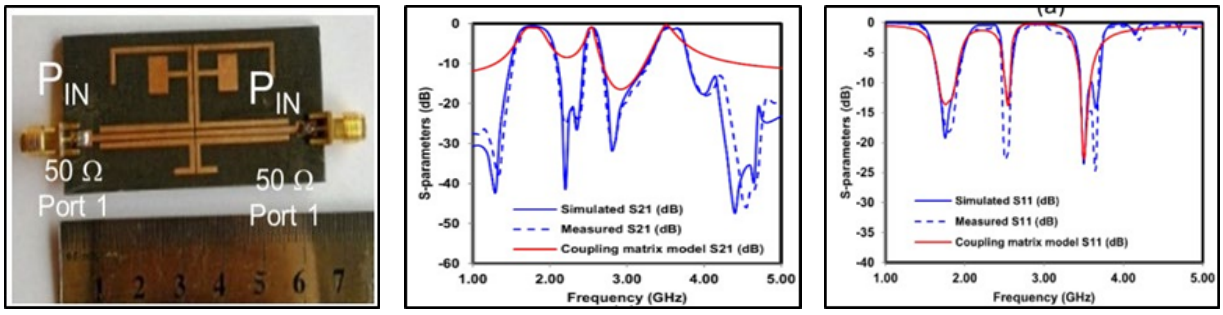

(a) **(b)**

Figure 24: (a)The prototype of the suggested design, and (b) Measured and simulated findings comparison

Chang, Wei-Chung, and Wen-Hua Tu. [41] presented a dual-band bandpass filter capable of achieving remarkable performance, using various implementation methods like as microstrip, coplanar, multilayer microstrip, and SIW. Filters are rated based on their figure of merit (FoM), which is indicated as the transmission coefficient level, selectivity, spurious-free response, and size. To get the best FoM, three possible dual-band BPFs with various feeding technologies, resonators, and design topologies are studied. . Figure 25(a) shows the prototype of the suggested design; and Figure 25(b) shows the measured and simulated results comparison.

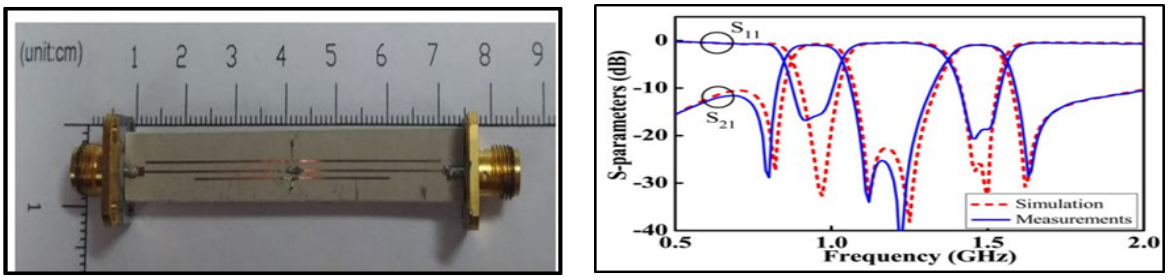

(a) **(b)**

Figure 25: (a) The prototype of the suggested design, and (b) Measured and simulated results comparison

Tantiviwat, Sugchai, et al. [42] presented microstrip quad-band BPF with flexible control for DCS, WLAN, WiMAX, and 5G applications. Both the first and second passbands are obtained using two dual-mode short-circuited SLRs that share a via-hole, the third passband is produced by using λg/2 coupled-line resonator. At the fourth passband, a second dual-mode open-circuited SLR can be used. The frequencies of the presented design are 1.80/2.45/3.50/4.90 GHz. It is possible to vary each passband separately with little impact on the other passbands. Furthermore, by adjusting the coupling parameters, the bandwidth of each passband may be freely regulated. The presented structure has a size of 0.024 λg2. The measurements are in good accord with the findings of simulations. In each of the four passbands, the measured reflection coefficients are at least 12 dB. Figure 26(a) shows the prototype of the suggested design; and Figure 26(b) shows the measured and simulated results comparison. The performance comparisons for recent microstrip mixed-band BPFs for 5G applications are listed in Table 4.

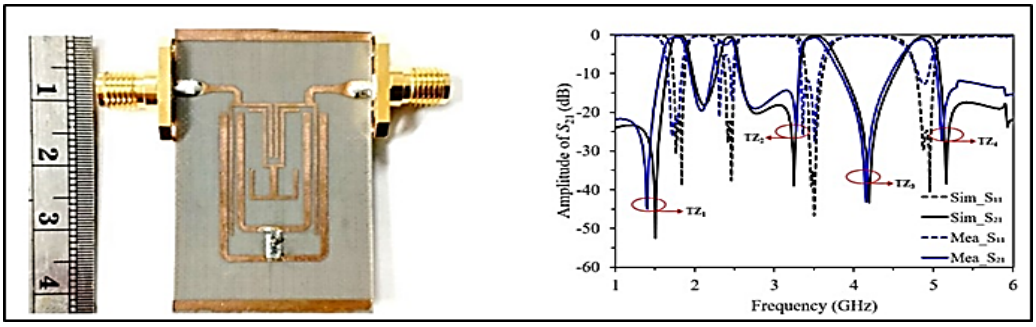

(a) **(b)**

Figure 26: (a) The prototype of the suggested design, and (b) Measured and simulated results comparison

Table 4: Tables Performance comparisons for recent microstrip mixed-band BPFs for 5G Applications

Technology	Substrate	Freq. (GHz)	FBW (%)	$\|S_{21}\|$ (dB)	$\|S_{11}\|$ (dB)	Size (λg^2) or(mm^2)	IS (dB)	TZs	IBs	Applications	Ref.
novel multi-stub loade	RO4003C	2.4\3.5\ 5.45	11.6\6.7\ 17.8	1.1\1.2\1	>15	0.023 λg^2	>-30\>-30	4	NA	5G WiFi Application	[36]
multi-stub loaded	RO4003C	1.8\2.45\ 3.5\5.5	6.7\4.2\ 3.7\14.8	1.5\1.7\ 2.3\1.8	>15	0.028 λg^2	>-30\>-40\>-50	6	Yes\ no\yes\no	DCS/WLAN/WiMAX/5G Wi-Fi Application	[37]
Half-wavelength step impedance	FR4	2.45\5.45	22.8\8.6	-	>20\>15	-	>-40	4	NA	WLAN and 5G Wi-Fi Applications	[38]
planer open-loop	RO3010	2.55\ 3.65	3.9\2.7	-	10	0.045 λg^2	>-40	2	NA	4G and 5G applications	[7]
SL-UIRs	Duroid 5880	2.4\3.5\5.2	4.22\3.98 \3.43	1.76\0.95\ 1.5	17.3\25.3 \19.8	0.025 λg^2	>-30\>-40	6	NA	WLAN and 5G	[39]
Multi-Coupled Line Stub-SIR	RT/Duroid 5880	1.75\2.55 \3.55	21.2\4.7\ 8.4	0.55\1.36\ 1.37	>15\>20\ >20	0.038 λg^2	>-30\>-40	6	yes	WCDMA \WLAN\WiFi) \ LTE\5G communication	[40]
SIR with a loaded open-circuited stub.	RT/Duroid 6010LM	0.95\ 1.47		1\1.2	>15	-	>-30	4	NA	software-defined radio and 5G	[41]
dual-mode short-circuited SLRs\ coupled-line	Diclad Arlon 880	1.80/2.45 /3.50/4.9	13.74/4.52/8.3/5.80	0.65/1.42/ 0.78/1.2	>20\>5\>10\>10	0.024 λg^2	>-15\>-40\>-40	4	yes	DCS/WLAN/WiMAX and 5G applications	[42]

7. Conclusion

This article provides up-to-date extensive reviews of microstrip single/multi-band bandpass filter designs, methodologies, and problems for 5G applications. The study includes single/multiband microstrip BPFs that use various design techniques for present and future 5G applications. This study also presents and discusses a comparison of alternative design techniques and layouts while focusing on the most important parameters of microstrip BPFs. We derived the major challenges from these reviews, which included the size, performance, and individuality of microstrip BPFs filters. Despite certain limitations, we expect to see more novel, exciting, and versatile BPFs in the next years.

Author contribution

All authors contributed equally to this work.

Funding

This research received no specific grant from any funding agency in the public, commercial, or not-for-profit sectors.

Data availability statement

The data that support the findings of this study are available on request from the corresponding author.

Conflicts of interest

The authors declare that there is no conflict of interest.

References

[1] N. Sahayam, A Review on Microstrip Filter for the Application in Communication System, pp. 709–717, 2018.

[2] A. J. Malse and R. Kulshreshtha, A Survey on Narrowband filtering Design using Microstrip filters, Int. J. Eng. trends Technol., 34 (2016) 327–330.

[3] A. Abdel-Rahman, A. R. Ali, S. Amari, and A. S. Omar, Compact bandpass filters using Defected Ground Structure (DGS) coupled resonators, IEEE MTT-S Int. Microw. Symp. Dig., 2005 (2005) 1479–1482. https://doi.org/10.1109/MWSYM.2005.1516971

[4] J. Nieto and R. Sauleau, Miniature coplanar waveguide and microstrip stop-band filters using spiral resonators, Eur. Sp. Agency, (Special Publ. ESA SP, 626 (2006) 2–6. https://doi.org/10.1109/eucap.2006.4585014

[5] Y. I. A. Al-Yasir et al., Design of multi-standard single/tri/quint-wideband asymmetric stepped-impedance resonator filters with adjustable TZs, IET Microwaves, Antennas Propag., 13 (2019) 1637–1645. https://doi.org/ 10.1049/iet-map.2018.5863

[6] J. S. Hong and M. J. Lancaster, Couplings of microstrip square open-loop resonators for cross-coupled planar microwave filters, IEEE Trans. Microw. Theory Tech., 44 (1996) 2099–2109.

[7] Y. I. A. Al-Yasir, N. OjaroudiParchin, A. Abdulkhaleq, K. Hameed, M. Al-Sadoon, and R. Abd-Alhameed, Design, Simulation and Implementation of Very Compact Dual-band Microstrip Bandpass Filter for 4G and 5G Applications, SMACD 2019 - 16th Int. Conf. Synth. Model. Anal. Simul. Methods Appl. to Circuit Des. Proc., 2019,41–44. https://doi.org/10.1109/SMACD.2019.8795226

[8] J. Rajendran, Design and Optimization of Band Pass Filter for SoftwareDefined Radio Telescope, Int. J. Inf. Electron. Eng., 2 (2012) 649–651. https://doi.org/10.7763/ijiee.2012.v2.180

[9] H. N. Shaman, New S-band bandpass filter (BPF) with wideband passband for wireless communication systems, IEEE Microw. Wirel. Components Lett., 22 (2012) 242–244. https://doi.org/10.1109/LMWC.2012.2190269

[10] M. R. Saad et al., Designing 5GHz microstrip coupled line bandpass filter using LTCC technology, 2008 Int. Conf. Electron. Des. ICED .2008, 6–9. https://doi.org/10.1109/ICED.2008.4786774

[11] R. K. Maharjan and N. Y. Kim, Microstrip Bandpass Filters Using Window Hairpin Resonator and T-Feeder Coupling Lines, Arab. J. Sci. Eng., 39 (2014) 3989–3997. https://doi.org/10.1007/s13369-014-0997-7

[12] S. C. Lin, C. H. Wang, Y. W. Chen, and C. H. Chen, Improved combline bandpass filter with multiple transmission zeros, Asia-Pacific Microw. Conf. Proceedings, APMC. 2 ,2007,7–10. https://doi.org/10.1109/APMC.2007.4554864

[13] Y. M. Chen, S. F. Chang, C. C. Chang, and T. J. Hung, Design of stepped-impedance combline bandpass filters with symmetric insertion-loss response and wide stopband range, IEEE Trans. Microw. Theory Tech., 55 (2007) 2191–2198. https://doi.org/10.1109/TMTT.2007.906482

[14] D. Psychogiou, R. Gómez-García, and D. Peroulis, RF Wide-Band Bandpass Filter With Dynamic In-Band Multi-Interference Suppression Capability, IEEE Trans. Circuits Syst. II Express Briefs, 65 (2018) 898–902. https://doi.org/10.1109/TCSII.2017.2726145

[15] Q. Cai, Y. Li, X. Zhang, and W. Shen, Wideband MIMO Antenna Array Covering 3.3-7.1 GHz for 5G Metal-Rimmed Smartphone Applications, IEEE Access, 7 (2019)142070–142084. https://doi.org/10.1109/ACCESS.2019.2944681

[16] S. B. Patel and M. Kansara, Comparative Study of 2G , 3G and 4G, no. September, 2018.

[17] S. B. E. N. Haddi, A Compact Microstrip T-Shaped Resonator Band Pass Filter for 5G Applications, Int. Conf. Intell. Syst.Comput. Vision , 2020, 1-5. https://doi.org/10.1109/ISCV49265.2020.9204054

[18] and T. N. Harri Holma, Antti Toskala, 5G Technology: 3GPP New Radio. 2020.

[19] A. O. Watanabe et al., A Review of 5G Front-End Systems Package Integration, IEEE Trans. Compon. Packag. Manuf. Technol., 11 (2021) 118-133.https://doi.org/10.1109/TCPMT.2020.3041412

[20] M. Caleffi, S. Member, V. Trianni, A. S. Cacciapuoti, and S. Member, Self-Organizing Strategy Design for Heterogeneous Coexistence in the Sub-6 GHz, IEEE Trans. Wireless Commun., 17 (2018) 7128-7143. https://doi.org/10.1109/TWC.2018.2864734

[21] N. N. Al-Areqi, N. Seman, and T. A. Rahman, Parallel-coupled line bandpass filter design using different substrates for fifth generation wireless communication applications, 2015 Int. Symp. Antennas Propagation, ISAP 2015. 2015, 2016,1–5.

[22] Y. Al-Yasir, R. A. Abd-Alhameed, J. M. Noras, A. M. Abdulkhaleq, and N. O. Parchin, Design of very compact combline band-pass filter for 5G applications, IET Conf. Publ., 2018, CP746, 2018. https://doi.org/10.1049/cp.2018.1482

[23] Y. I. A. Al-Yasir et al., Design, simulation and implementation of very compact open-loop trisection BPF for 5G communications, 2019 IEEE 2nd 5G World Forum (5GWF), Dresden, Germany, 2019, 189-193. https://doi.org/10.1109/5GWF.2019.8911677

[24] S. Saleh, W. Ismail, I. S. Zainal Abidin, and M. H. Jamaluddin, 5G Hairpin and Interdigital Bandpass Filters, Int. J. Integr. Eng., 12 (2020) 71–79. https://doi.org/10.30880/ijie.2020.12.06.009

[25] F. M. Alnahwi, Y. I. A. Al-Yasir, A. A. Abdulhameed, A. S. Abdullah, and R. A. Abd-Alhameed, A low-cost microwave filter with improved passband and stopband characteristics using stub loaded multiple mode resonator for 5g mid-band applications, Electron., 10 (2021) 1–15. https://doi.org/10.3390/electronics10040450

[26] Q. Abdullah et al., A Compact Size 5G Hairpin Bandpass Filter with Multilayer Coupled Line, Comput. Mater. Contin., 69 (2021) 4025–4042. https://doi.org/10.32604/cmc.2021.018798

[27] A. Basheer, H. Abdulhussein, H. Al-Saedi, and J. K. Ali, Design of Bandpass Filter for 5G Applications with High-selectivity and Wide Band Rejection, (2022)179–183. https://doi.org/10.1109/micest54286.2022.9790185

[28] M. Riaz, B. S. Virdee, P. Shukla, K. Ouazzane, M. Onadim, and S. Salekzamankhani, Quasi-elliptic dual-band planar BPF with high-selectivity and high inter-band isolation for 5G communications systems, Microw. Opt. Technol. Lett., 62 (2020) 1509–1515. https://doi.org/10.1002/mop.32197

[29] W.-L. Hsu, P.-Y. Lyu, and S.-F. Chang, Design of a miniature dual-band bandpass filter with interlocked stepped-impedance resonators for 5G new radio access technology, Int. J. Microw. Wirel. Technol., 12 (2020) 733–737.

[30] W. Zhang, K. Ma, H. Zhang, and H. Fu, Design of a Compact SISL BPF with SEMCP for 5G Sub-6 GHz Bands, IEEE Microw. Wirel. Components Lett., 30 (2020) 1121–1124. https://doi.org/10.1109/LMWC.2020.3030189

[31] J. Peng, Z. Xu, J. Zhu, Design of Dual-Band Bandpass Filter Using a Hybrid Feed Scheme, 2020 Cross Strait Radio Sci. Wirel. Technol. Conf. CSRSWTC 2020 - Proc., 2,2020,16–18. https://doi.org/10.1109/CSRSWTC50769.2020.9372615

[32] H. I. Khani and A. S. Ezzulddin, Design of A Compact Dual-Band BPF for 5G Mobile Communications Using Folded $\lambda \mathrm{g}/2$ -Line Resonators, 71 (2022) 71–76. https://doi.org/10.1109/micest54286.2022.9790180

[33] Z. Hou et al., Dual-/Tri-wideband bandpass filter with high selectivity and adjustable passband for 5G mid-band mobile communications, Electron., vol. 9 (2020). https://doi.org/10.3390/electronics9020205

[34] H. I. Khani, A. S. Ezzulddin, H. Al-saedi, Design of a Compact and Highly Independent Triple- Band BPF for 5G Applications, Int. J. Microw. Opt. Technol., 17 (2022) 524–532.

[35] H. I. Khani, A. S. Ezzulddin, H. Al-saedi, Design of High-Selectivity Compact Quad-Band BPF Using Multi-Coupled Line and Short Stub-SIR Resonators, Prog. Electromagn. Res., 122 (2022) 215–228.

[36] L. Gao, X. Y. Zhang, and Q. Xue, Compact tri-band bandpass filter using novel eight-mode resonator for 5G WiFi application, IEEE Microw. Wirel. Components Lett., 25 (2015) 660–662.

[37] Y. Zhang, L. Gao, and X. Y. Zhang, Compact quad-band bandpass filter for DCS/WLAN/WiMAX/5G Wi-Fi application, IEEE Microw. Wirel. Components Lett., 25 (2015) 645–647.

[38] P. Khundrakpam, M. Pal, P. Sarkar, and R. Ghatak, A dual wideband bandpass filter for WLAN and 5G Wi-Fi applications, 2016 International Conference on Microelectronics, Computing and Communications (MicroCom), Durgapur, India, 2016,. 1-4. https://doi.org/10.1109/MicroCom.2016.7522575

[39] K. J. Lin, Z. F. Li, T. C. Tai, H. W. Wu, Y. H. Wang, A Compact Triple Passband Bandpass Filter Using Stub Load - Uniform impedance Resonators, Int. Symp. Signal Process. Commun. Syst., 2019, 1-2. https://doi.org/10.1109/ISPACS48206.2019.8986364

[40] T. Firmansyah, M. Alaydrus, Y. Wahyu, E. T. Rahardjo, and G. Wibisono, A highly independent multiband bandpass filter using a multi-coupled line stub-sir with folding structure, IEEE Access, 8 (2020) 83009–83026. https://doi.org/10.1109/ACCESS.2020.2989370

[41] W. C. Chang and W. H. Tu, Dual-band bandpass filter for software defined radio and 5G, Int. J. Microw. Wirel. Technol., 12 (2020) 629–634. https://doi.org/10.1017/S175907872000080X

[42] S. Tantiviwat, S. Z. Ibrahim, M. S. Razalli, and P. J. Soh, Design of Quad-Band Bandpass Filter Using Dual-Mode SLRs and Coupled-Line for DCS/WLAN/WiMAX and 5G Applications, Micromachines, 13 (2022) 2–9. https://doi.org/10.3390/mi13050700